Supporting information: Plague risk in the western United States over seven decades of environmental change

Last updated on October 11, 2021

Supplemental Figure 1: Summary model diagnostics for the wildlife plague risk model.

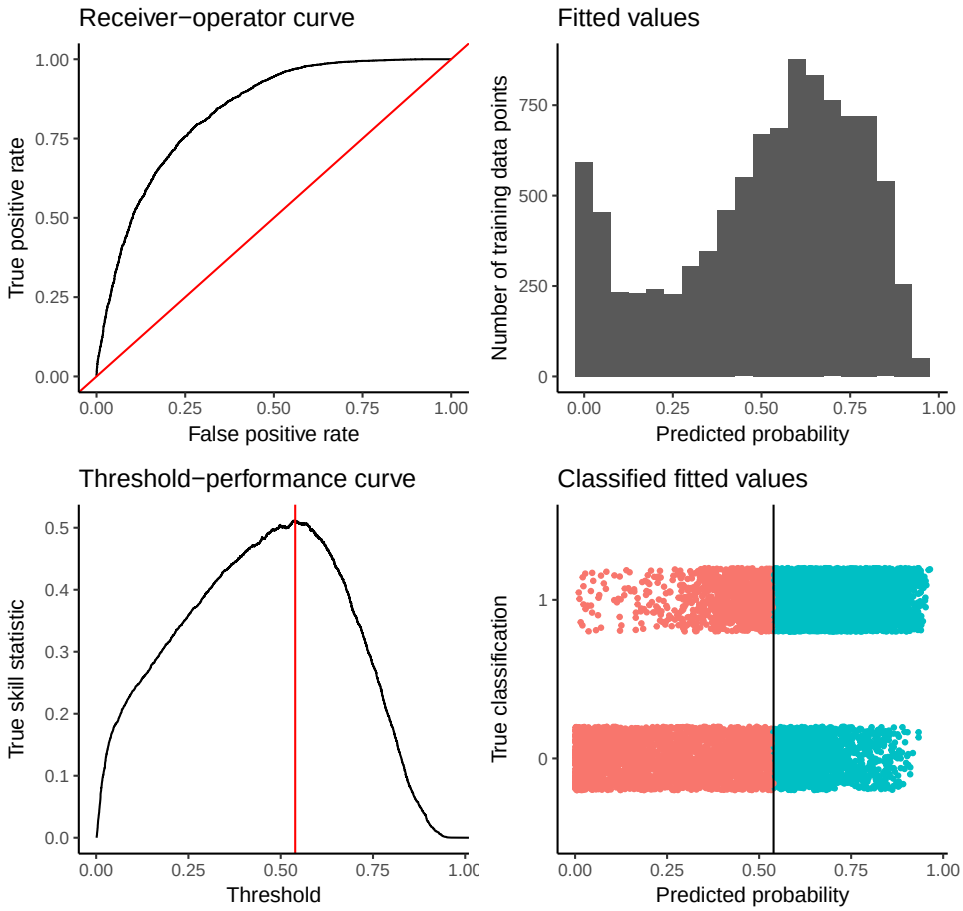

Supplemental Figure 2: Summary model diagnostics for the human plague risk model.

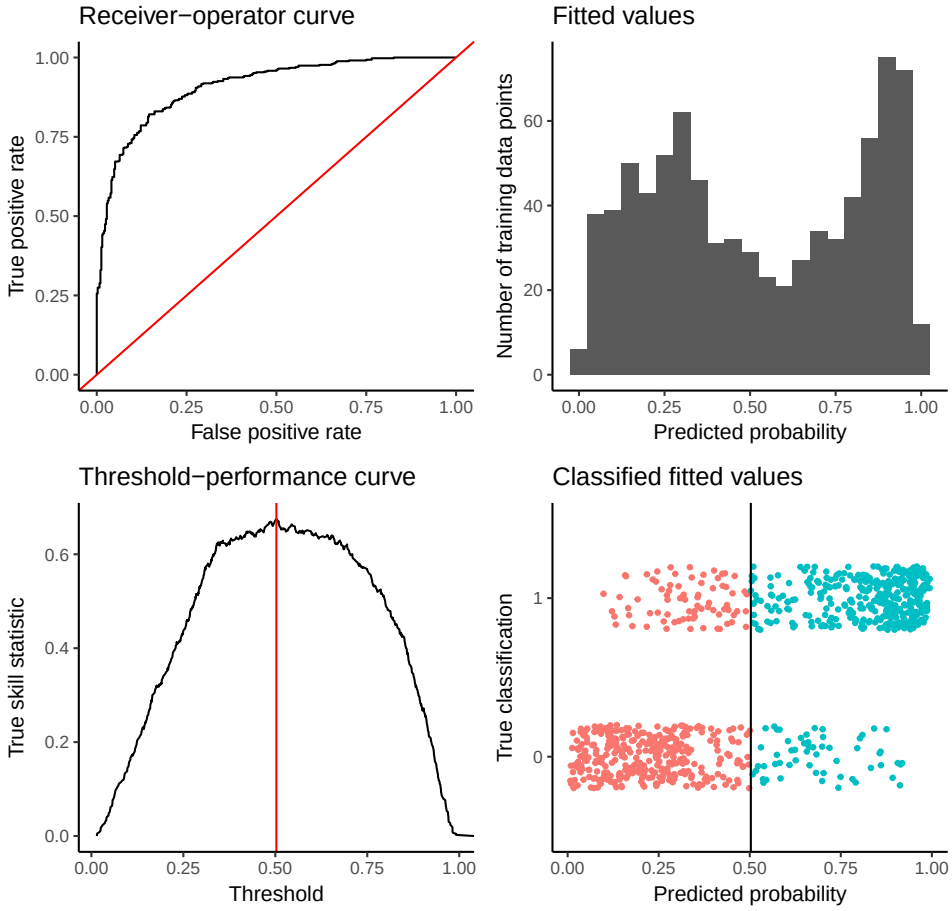

Supplemental Figure 3: Variable importance in the wildlife plague risk model. Variable name abbreviations are explained in Supplementary Table 1.

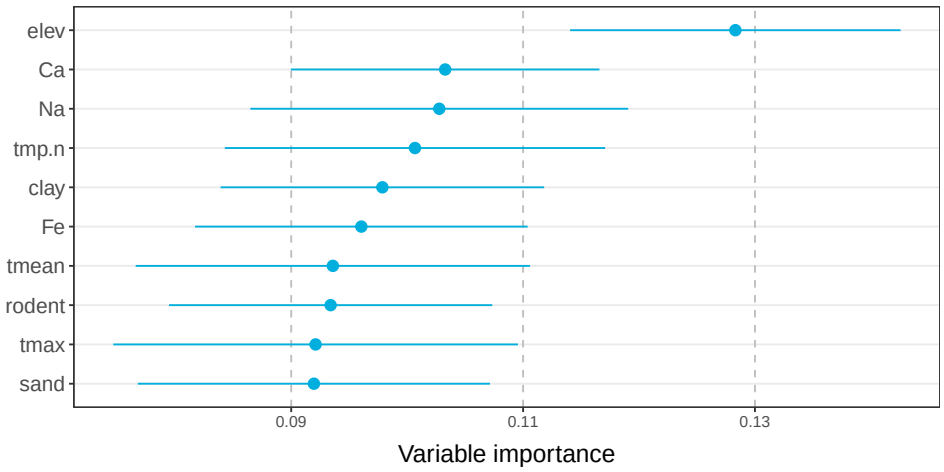

Supplemental Figure 4: Variable importance in the human plague risk model. Variable name abbreviations are explained in Supplementary Table 1.

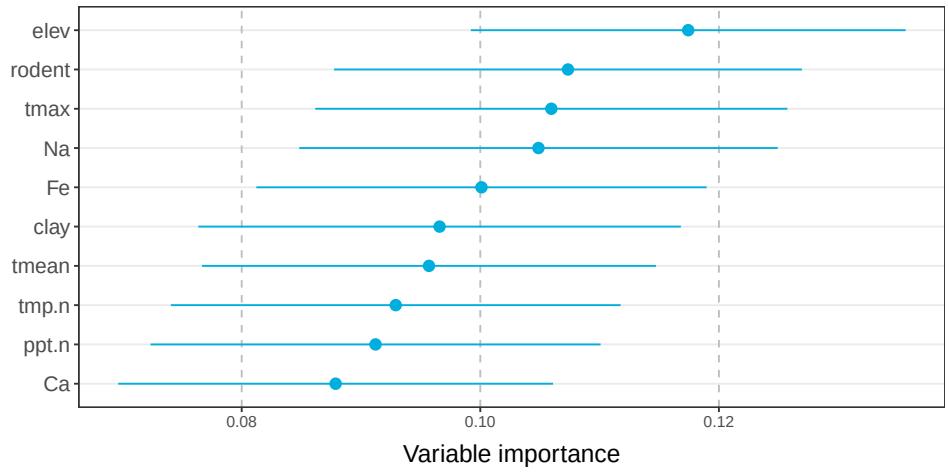

Supplemental Figure 5: The variable importance diagnostic for all variables considered for the wildlife plague risk model. Variable name abbreviations are explained in Supplementary Table 1.

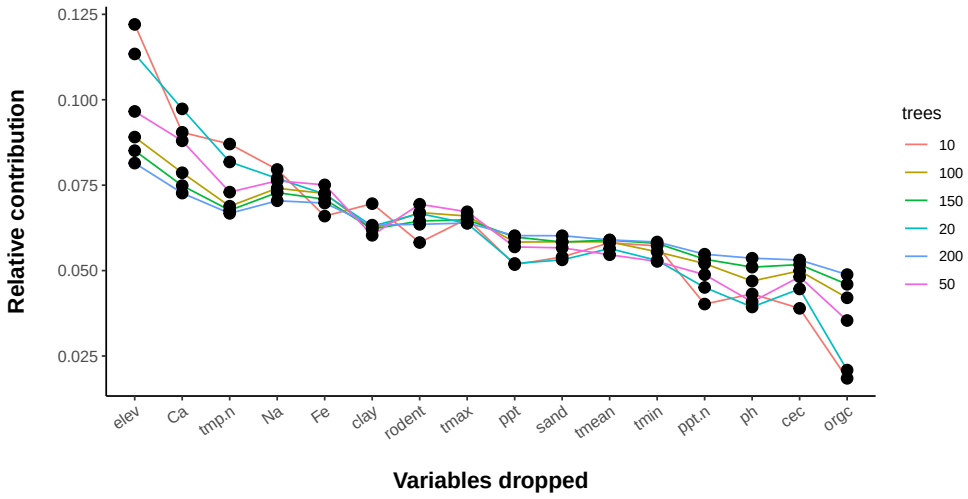

Supplemental Figure 6: The variable importance diagnostic for all variables considered for the human plague risk model. Variable name abbreviations are explained in Supplementary Table 1.

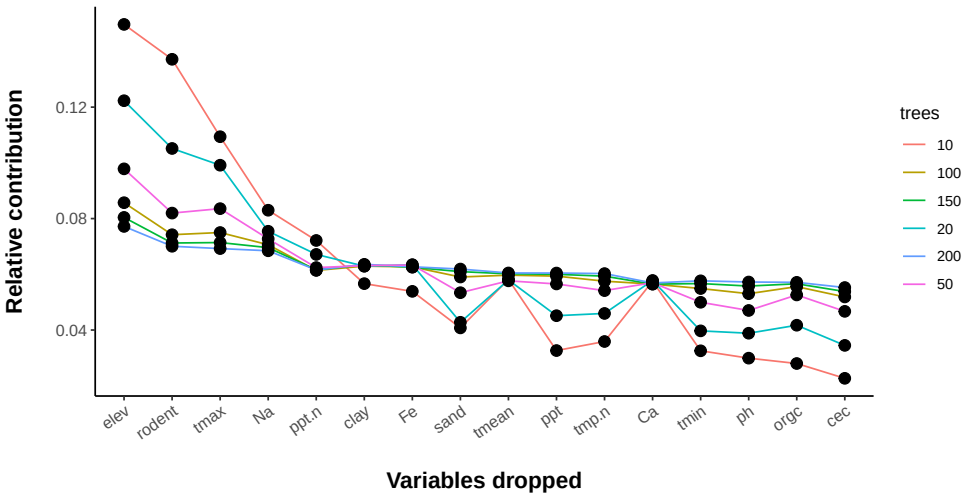

Supplemental Figure 7: Full partial dependence plots for the wildlife plague risk model. Partial dependence plots represent the relationship of a single variable to the predicted outcome, on a scale of 0 to 1, independent of the other variables fit in the model; blue shading gives a 95% credible interval from the posterior distribution of the Bayesian model. The steepness of these curves indicates the predicted magnitude of the effect, but not necessarily the variable's importance in the model. Variable name abbreviations are explained in Supplementary Table 1.

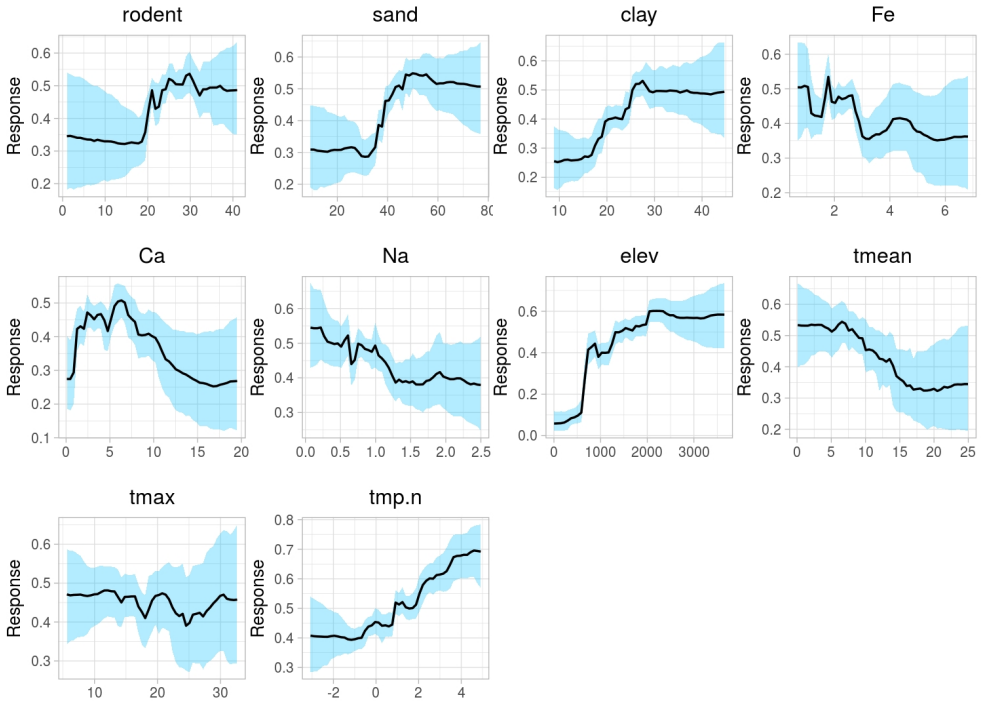

Supplemental Figure 8: Two-dimensional partial dependence plot for sand and clay in the wildlife model, projected onto the soil composition triangle as a ternary partial (tertial) dependence plot. Brighter colors (yellow) indicate a higher suitability for plague in that part of parameter space. Soils that are mostly sand, with some clay and minimal silt, are most suitable. Variable name abbreviations are explained in Supplementary Table 1.

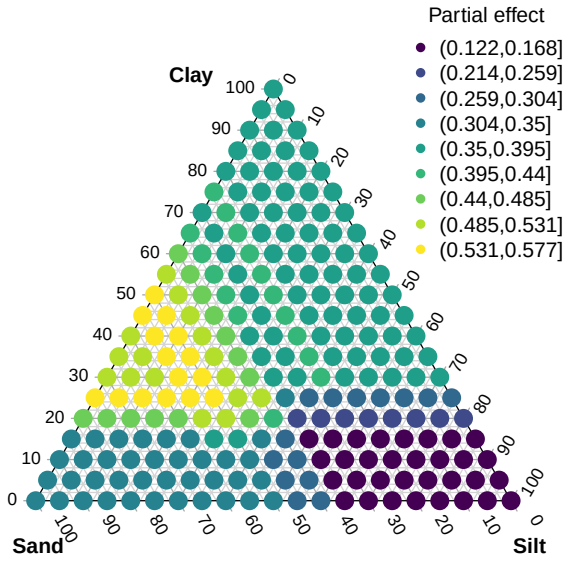

Supplemental Figure 9: Full partial dependence plots for the human plague risk model. Partial dependence plots represent the relationship of a single variable to the predicted outcome, on a scale of 0 to 1, independent of the other variables fit in the model; blue shading gives a 95% credible interval from the posterior distribution of the Bayesian model. The steepness of these curves indicates the predicted magnitude of the effect, but not necessarily the variable's importance in the model. Variable name abbreviations are explained in Supplementary Table 1.

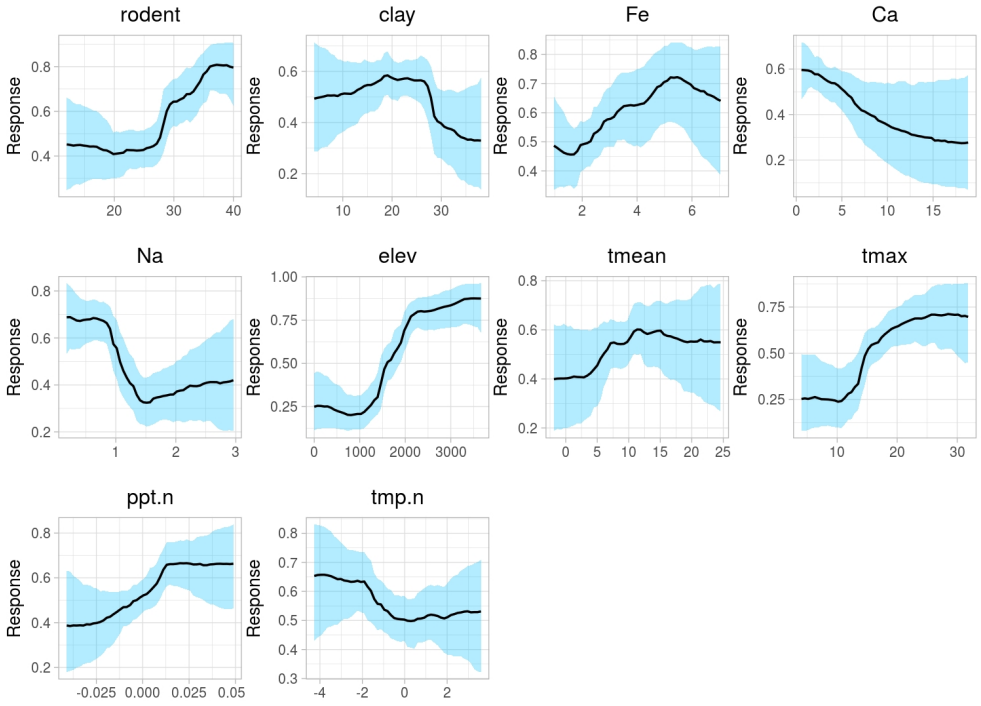

Supplemental Figure 10: Spatial partial (spartial) dependence plots for the wildlife plague risk model. Variables are given in descending order of model importance. Values are unitless partial effects on predicted probabilities that range from 0 to 1. Variable name abbreviations are explained in Supplementary Table 1.

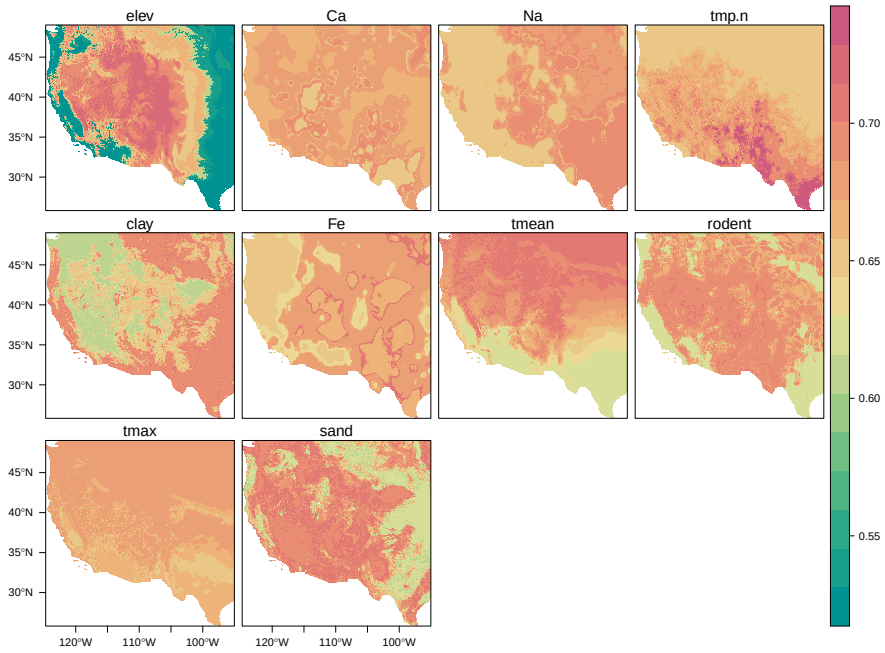

Supplemental Figure 11: Spatial partial (spartial) dependence plots for the human plague risk model. Variables are given in descending order of model importance. Values are unitless partial effects on predicted probabilities that range from 0 to 1. Variable name abbreviations are explained in Supplementary Table 1.

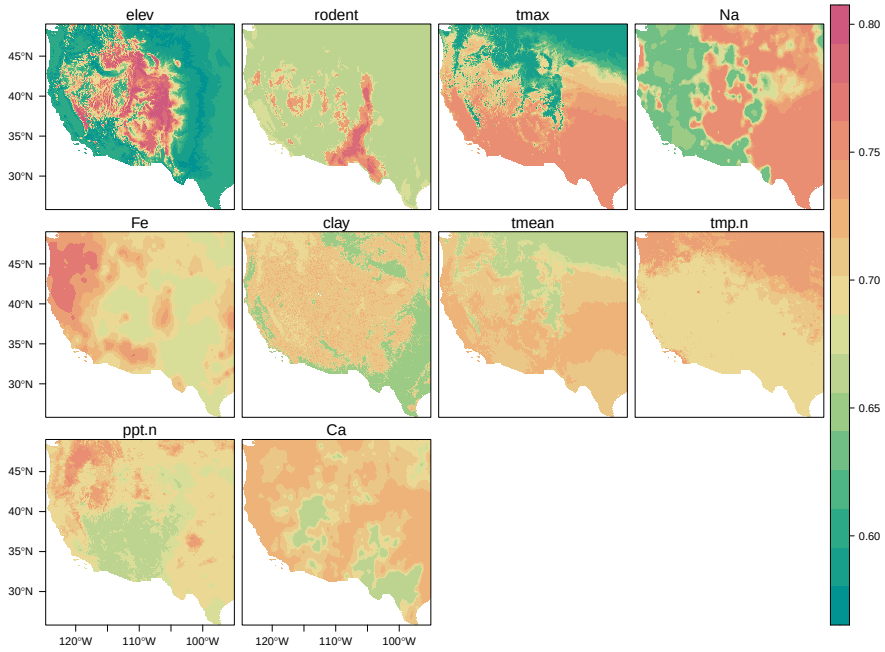

Supplemental Figure 12: Density of positive cases in the wildlife and human case data relative to recorded pH, modeled using a simple Loess smooth. (Values multiplied by 10 in the raw data.)

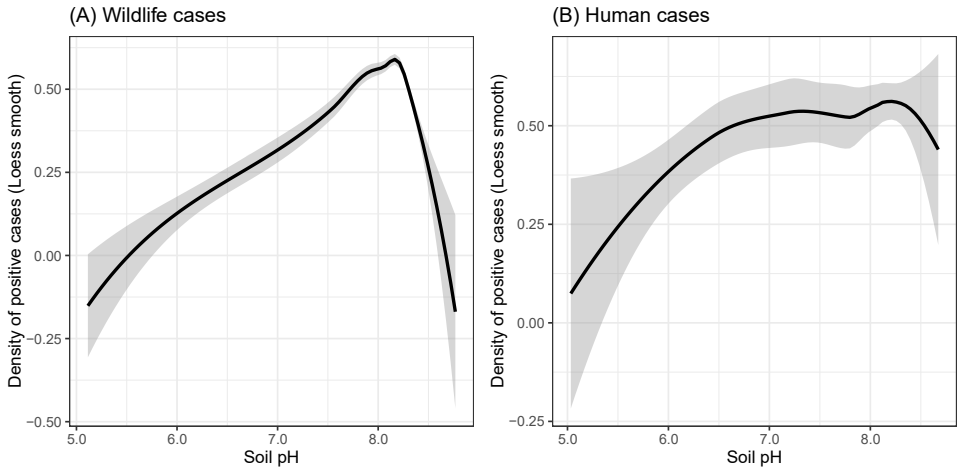

Supplemental Figure 13: Random intercept values for each year in the detection model for wildlife plague risk.

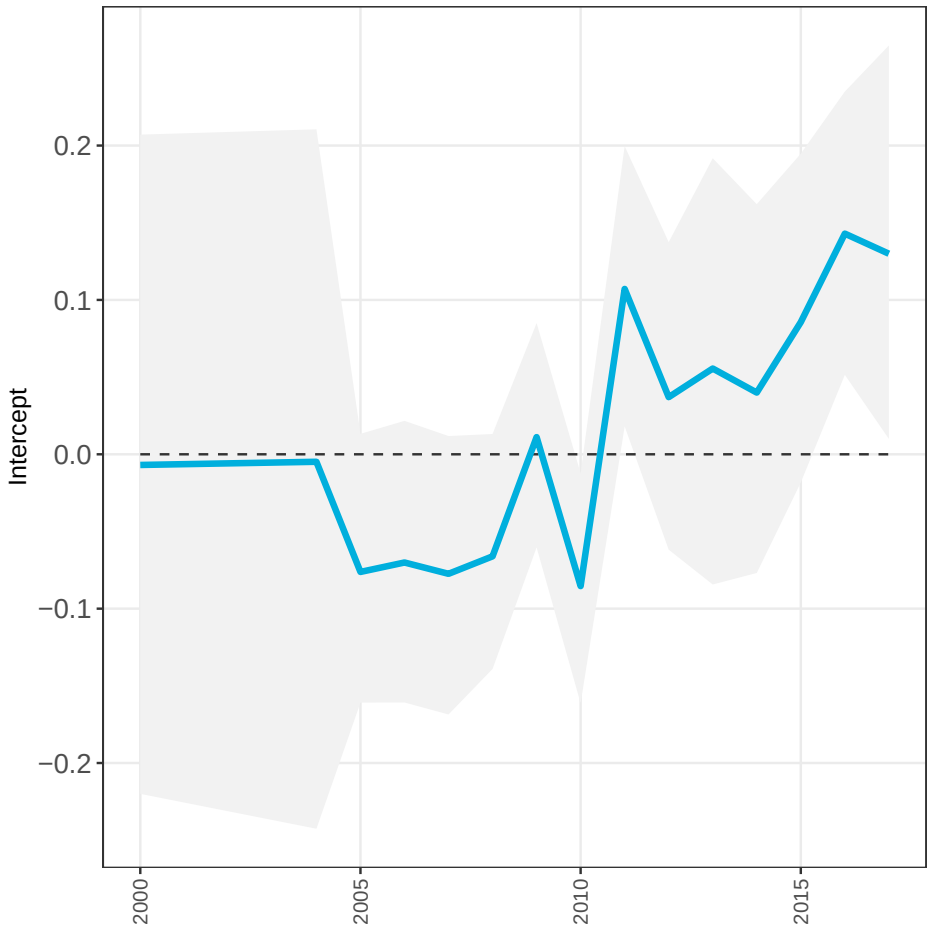

Supplemental Figure 14: Random intercept values for each year in the detection model for human plague risk.

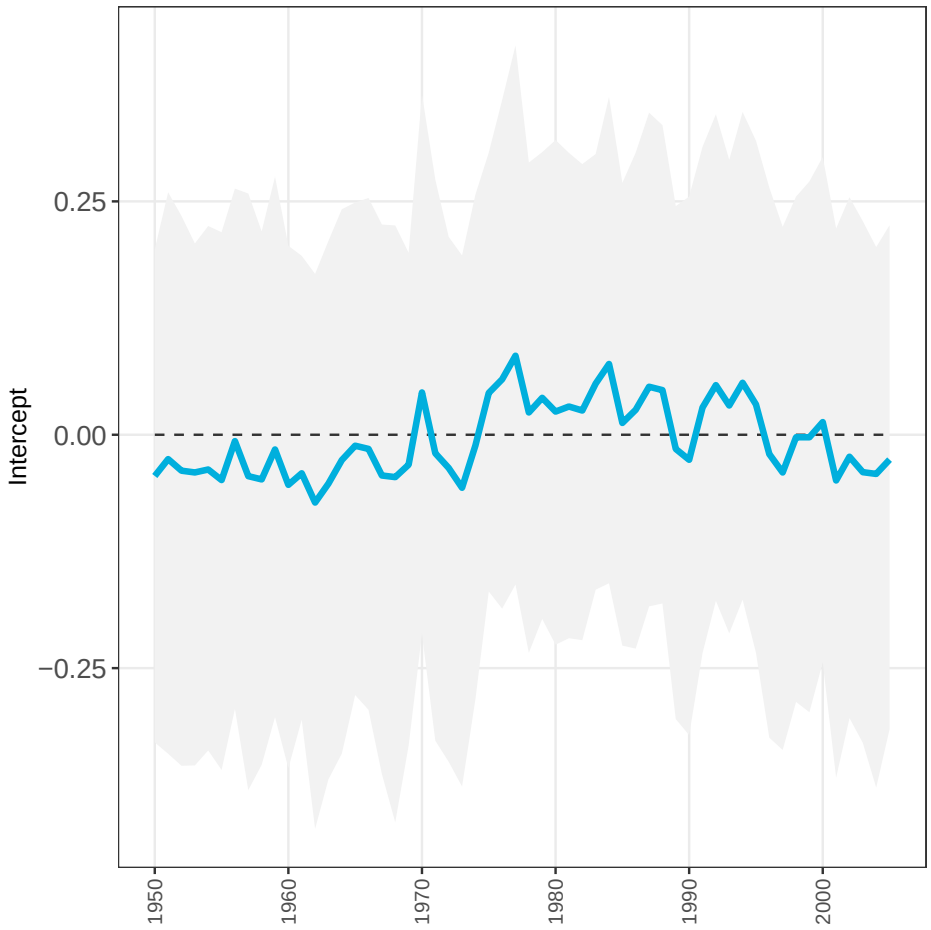

Supplemental Figure 15: Mean environmental suitability across years in the detection model (left: human; right: wildlife). Random intercept models have nearly identical predictions to baseline models; the two are nearly perfectly correlated for humans ($r = 0.992$) and wildlife ($r = 0.969$).

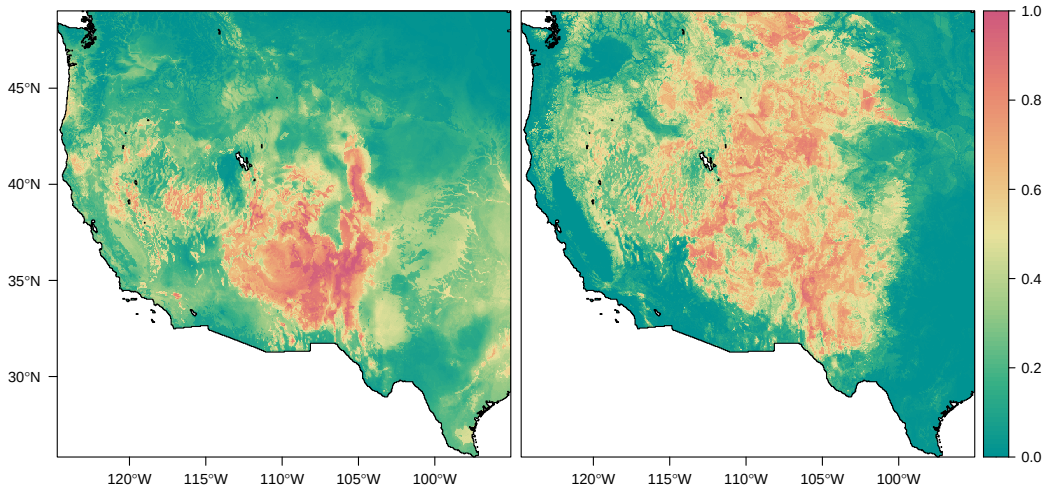

Supplemental Figure 16: Estimated percent change in plague suitability, 1950 to present, across pixels and the four main models. Red lines show the mean value.

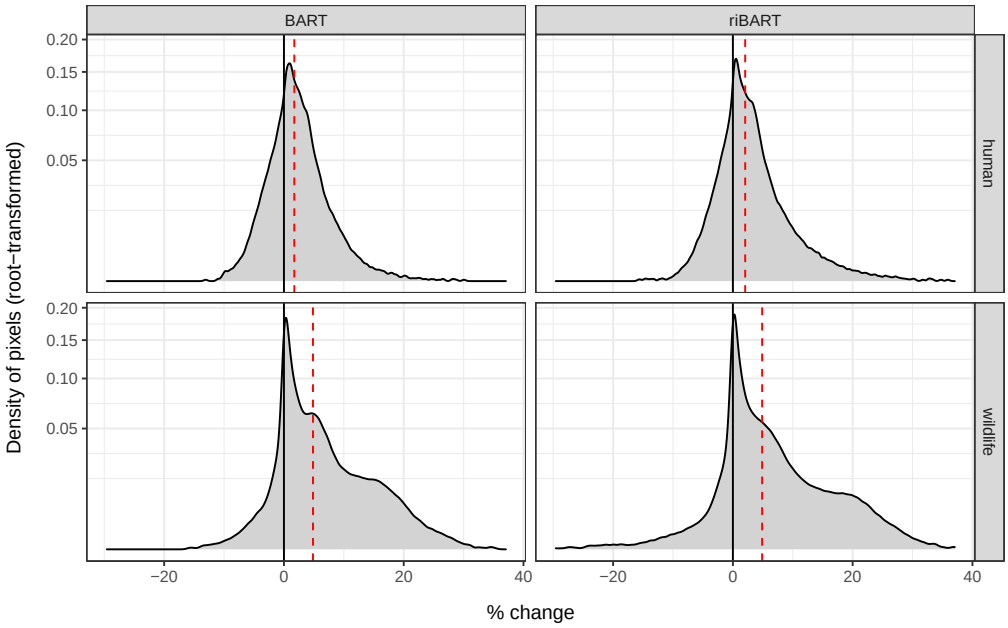

Supplemental Figure 17: Estimated percent change in plague suitability, 1950 to present, versus elevation.

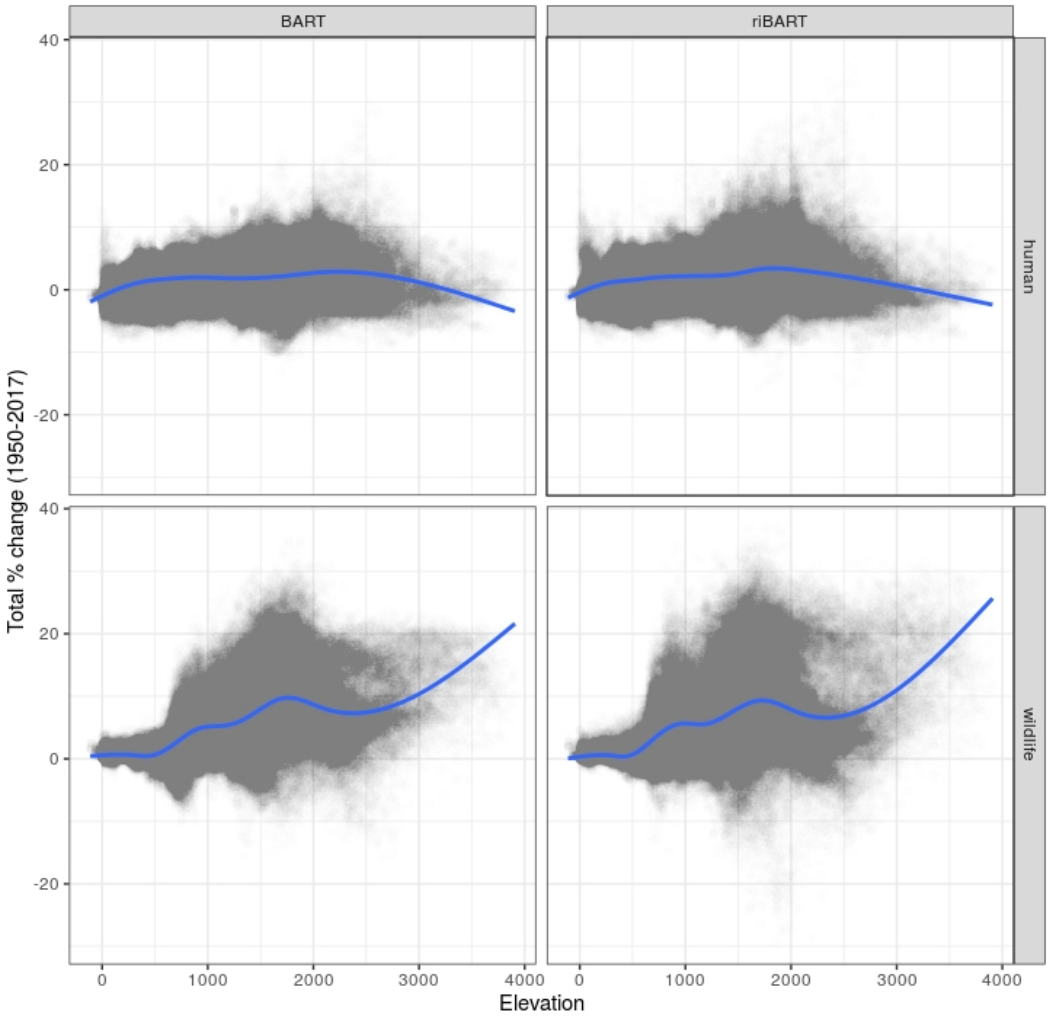

Supplemental Figure 18: Total estimated change in mean temperature, 1950 to present; the region as a whole experienced an average warming of 0.84 °C.

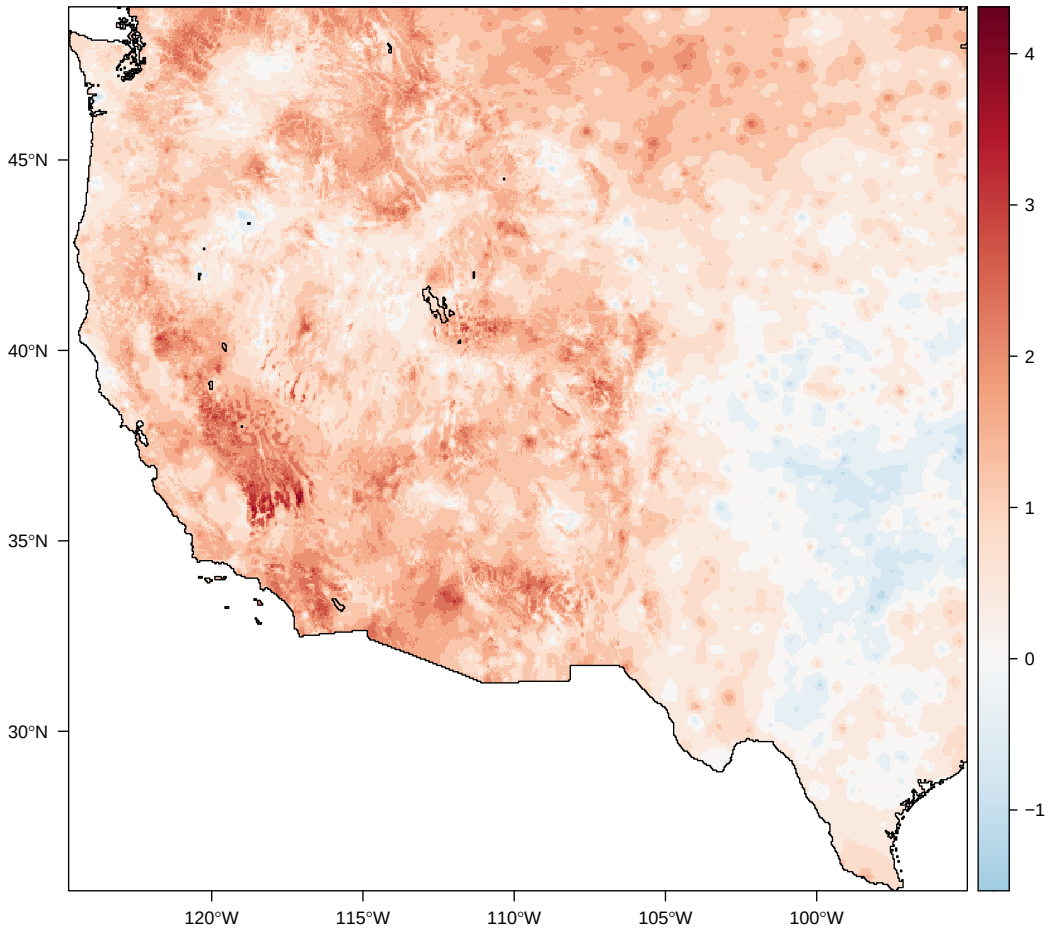

Supplemental Figure 19: Total estimated change in precipitation, 1950 to present; the region as a whole experienced an average increase of 41.7 mm of annual precipitation.

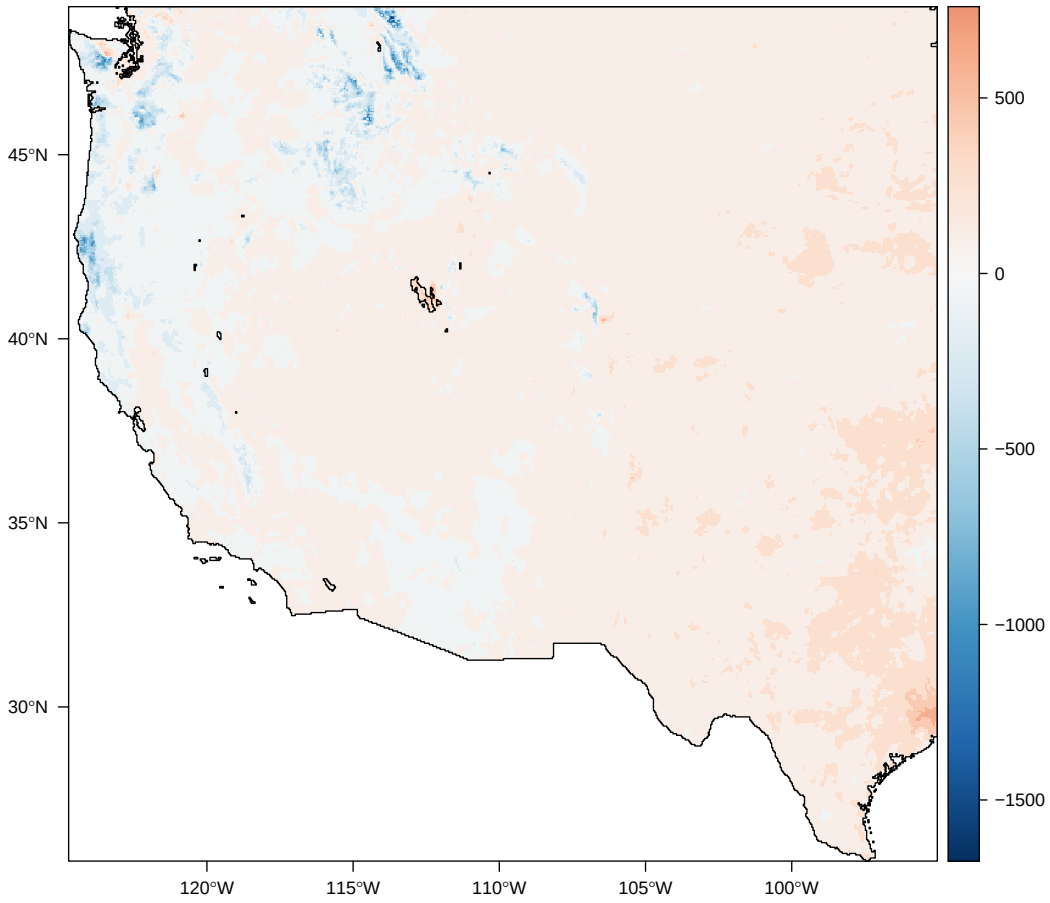

Supplemental Figure 20: Mean suitability for plague across all years (1950-2017), using the alternate human model (no variable set reduction).

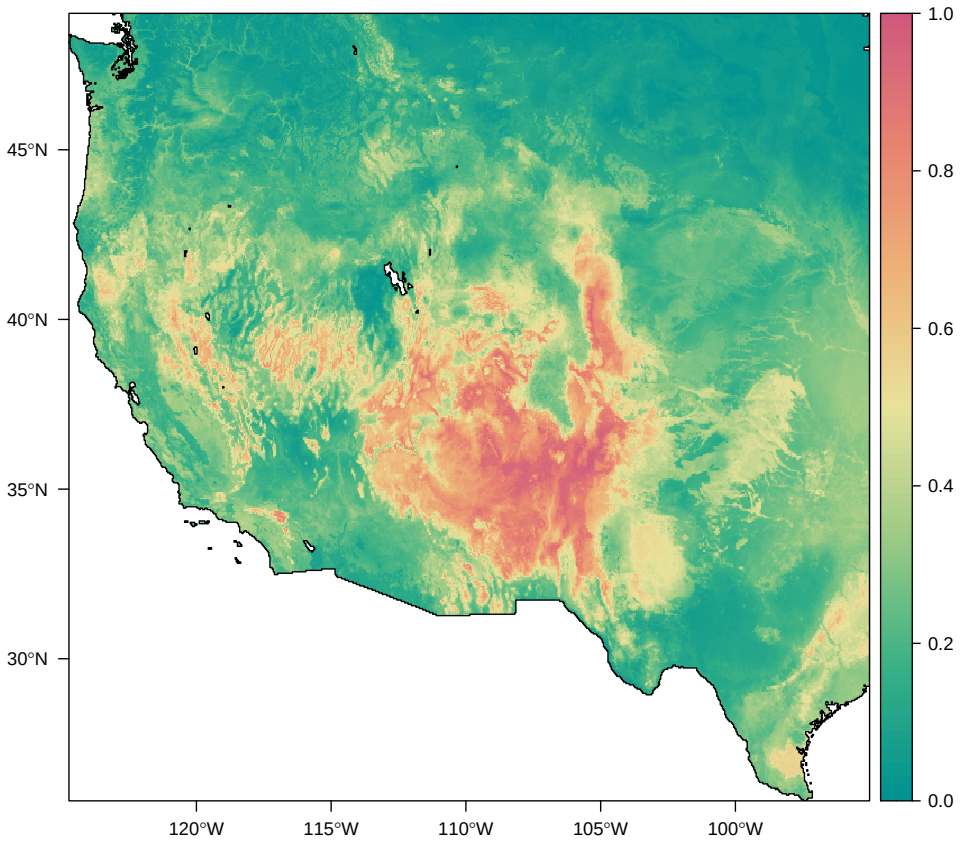

Supplemental Figure 21: The variable importance diagnostic for the alternate human model using the full variables set (no variable set reduction). Variable name abbreviations are explained in Supplementary Table 1.

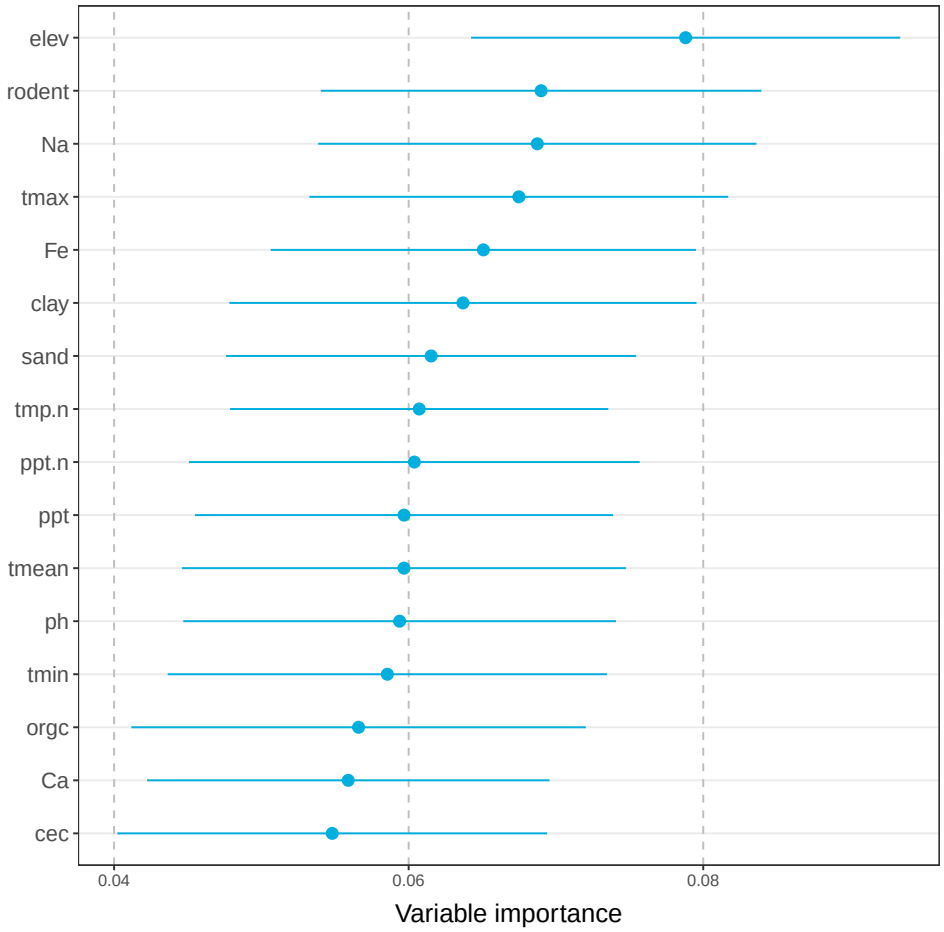

Supplemental Figure 22: Partial dependence plots for the alternate human model using the full variables set (no variable set reduction). Partial dependence plots represent the relationship of a single variable to the predicted outcome, on a scale of 0 to 1, independent of the other variables fit in the model; blue shading gives a 95% credible interval from the posterior distribution of the Bayesian model. The steepness of these curves indicates the predicted magnitude of the effect, but not necessarily the variable's importance in the model. Variable name abbreviations are explained in Supplementary Table 1.

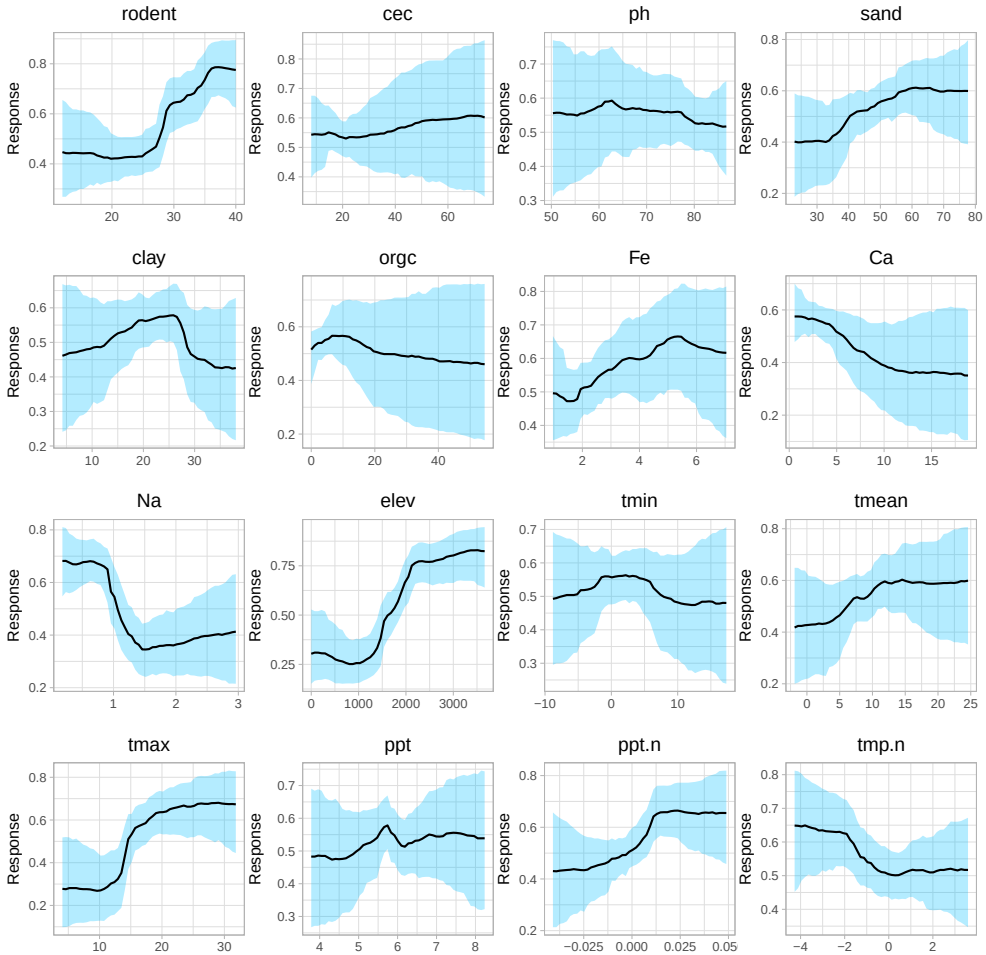

Supplemental Figure 23: Mean suitability for plague across all years (1950-2017), using the first alternate wildlife model (no variable set reduction).

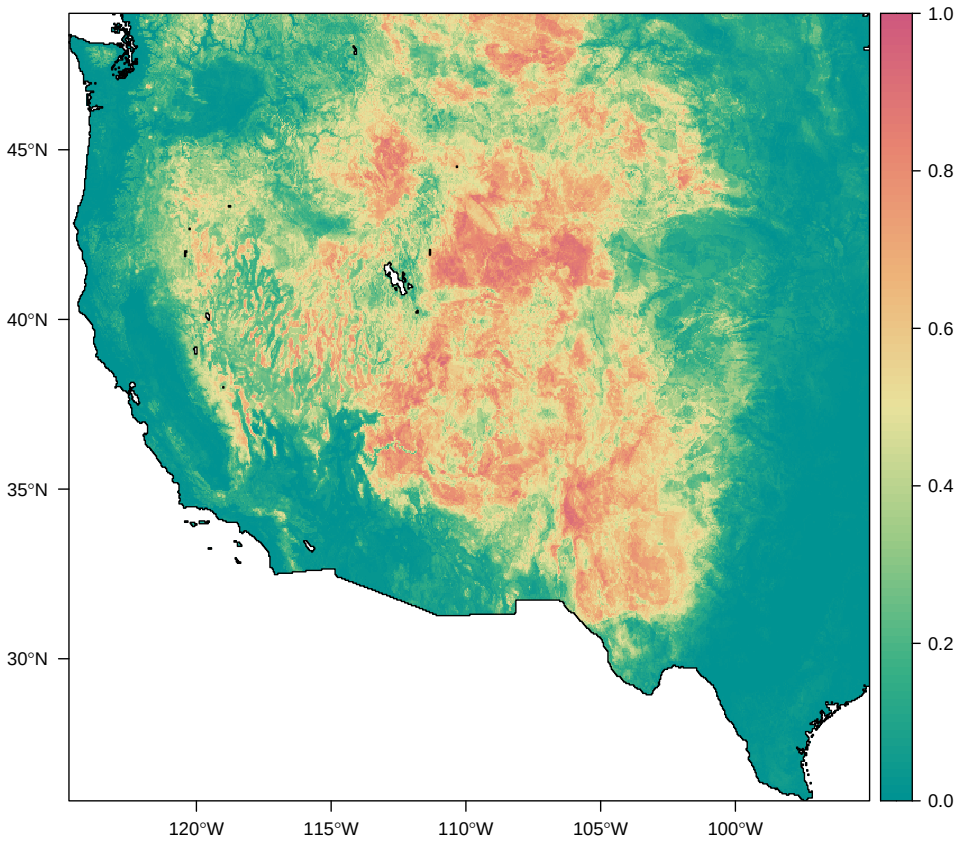

Supplemental Figure 24: The variable importance diagnostic for the first alternate wildlife model using the full variables set (no variable set reduction). Variable name abbreviations are explained in Supplementary Table 1.

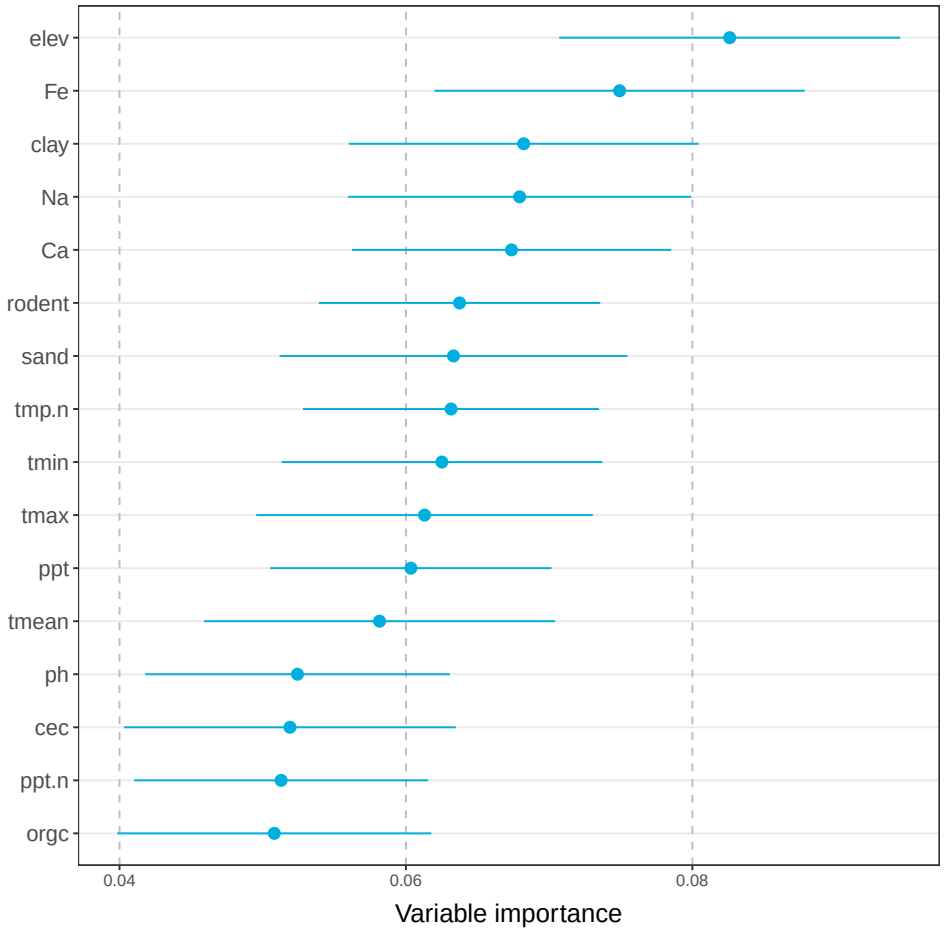

Supplemental Figure 25: Partial dependence plots for the alternate wildlife model using the full variables set (no variable set reduction). Partial dependence plots represent the relationship of a single variable to the predicted outcome, on a scale of 0 to 1, independent of the other variables fit in the model; blue shading gives a 95% credible interval from the posterior distribution of the Bayesian model. The steepness of these curves indicates the predicted magnitude of the effect, but not necessarily the variable's importance in the model. Variable name abbreviations are explained in Supplementary Table 1.

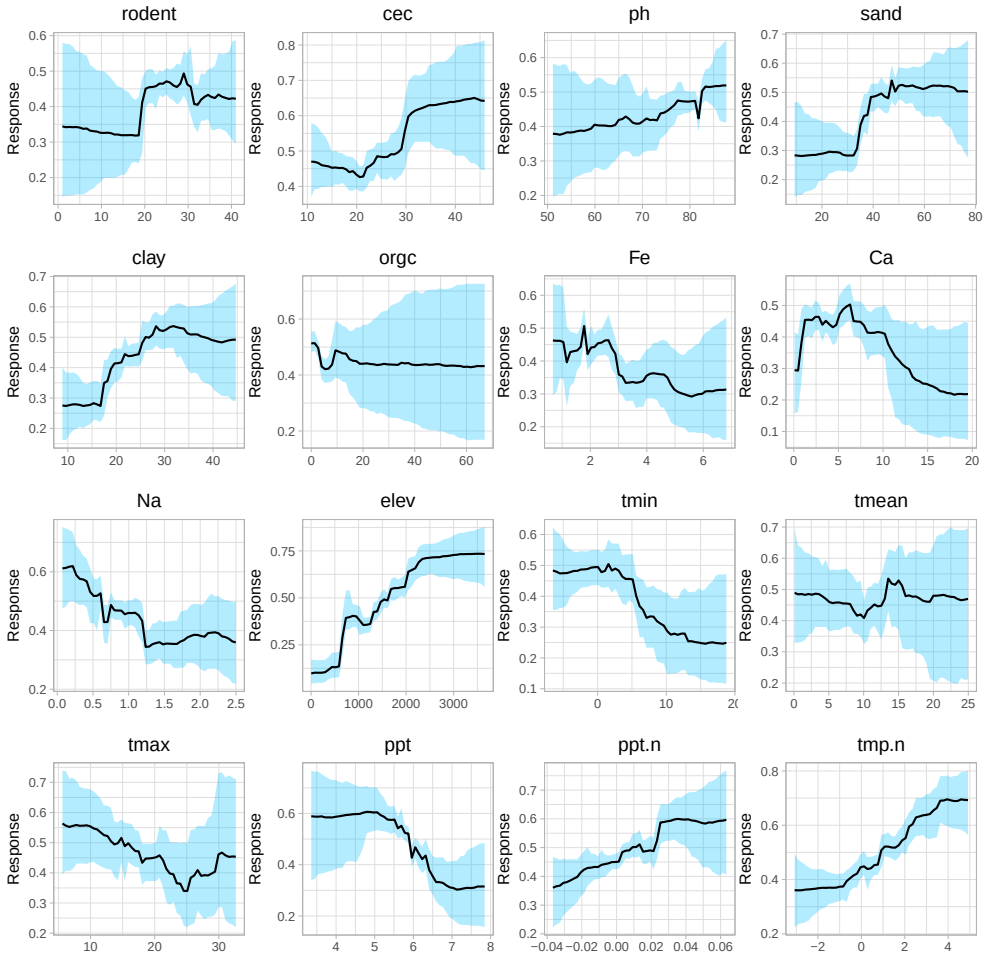

Supplemental Figure 26: Mean suitability for plague across all years (1950-2017), using the second alternate wildlife model (pseudoabsences instead of true absences).

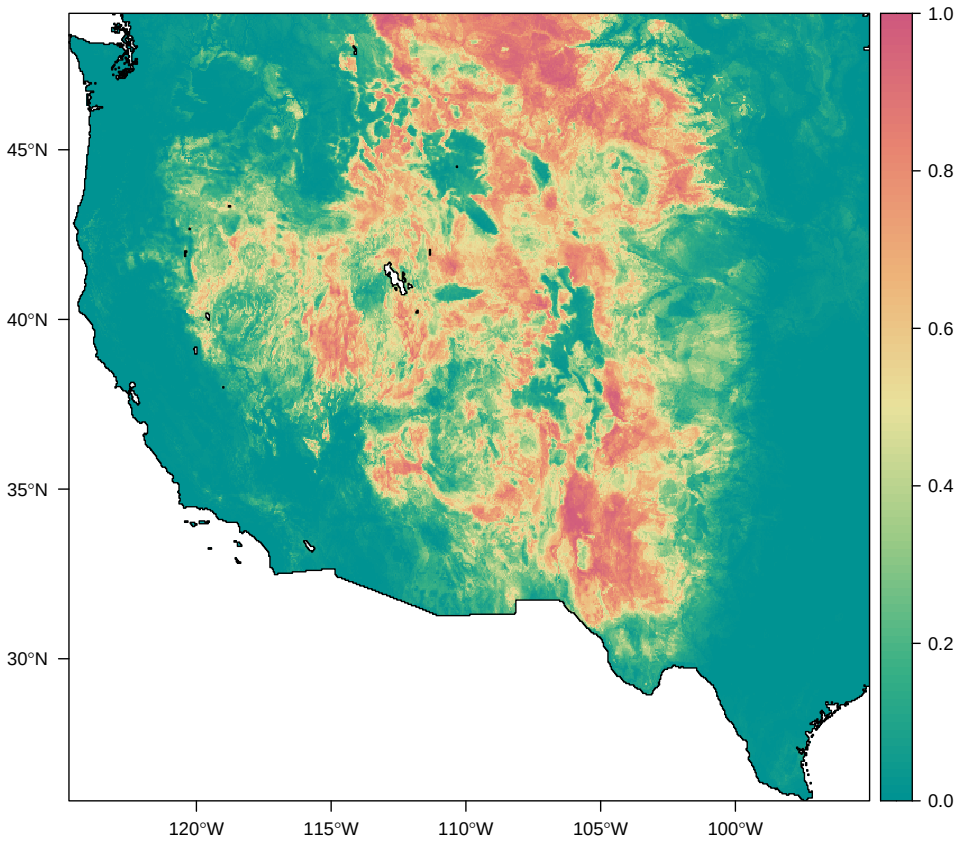

Supplemental Figure 27: Mean suitability for plague across all years (1950-2017), using the third alternate wildlife model (only coyote data).

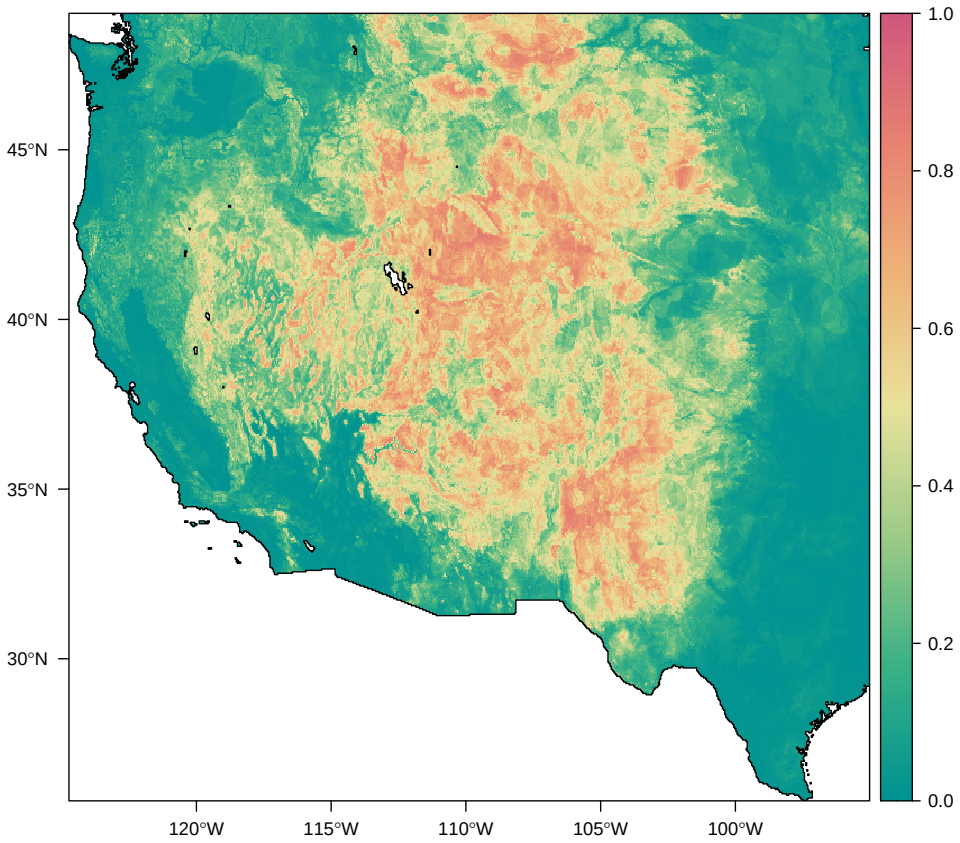

Supplemental Table 1: Variable name abbreviations used in this study, with full variable names and descriptions.

Variable	**Full variable name**
rodent	Rodent species richness
cec	Soil cation exchange capacity
ph	Soil pH (acidity)
sand	Soil percent sand content by volume
clay	Soil percent clay content by volume
org	Soil organic carbon content
Fe	Soil iron macronutrient concentration
Ca	Soil calcium macronutrient concentration
Na	Soil sodium macronutrient concentration ($\approx$ proxy for salinity)
elev	Elevation above sea level
tmin	Average minimum annual temperature
tmean	Mean annual temperature
tmax	Average maximum annual temperature
ppt	Mean annual precipitation
ppt.n	Annual normalized precipitation anomaly (relative to long-term average)
tmp.n	Annual normalized temperature anomaly (relative to long-term average)

Supplemental Table 2: Methodologies of previous studies applying ecological niche modeling to map plague (*Yersinia pestis*); this excludes studies focused on mapping individual reservoirs or fleas without any plague data. Abbreviations: PET/AET = potential and actual evapotranspiration; NDVI = normalized difference vegetation index; EVI = enhanced vegetation index; CTI = compound topographic index. † Note that this study also bootstrapped county level human cases in the U.S.

Study	Extent	Years	Algorithm	Predictors
1 †	USA	1965-2003?	GARP	Precipitation, temperature (min, mean, max), PET, AET, moisture surplus, moisture deficit, slope, aspect, elevation, CTI
2	Africa	1970-2007	GARP	BIO 1, 2, 5, 6, 12-14, slope, aspect, elevation, CTI, soil pH, soil moisture, soil carbon, PET, AET, humidity, growing degree days, NDVI
3	California, USA	1984–2004	MaxEnt	BIO 5, 7, 15-18
4	"North America"	Unspecified	Maxent	BIO 1, 2, 5, 6, 12-14
5	Western Usambara Mountains, Tanzania	1986-2003	GARP	EVI (mean, dry/rainy period means, standard error, seasonality, heterogeneity), slope, aspect, elevation, CTI
6	Northeast Brazil	1966–2011	GARP	BIO 1, 2, 5, 6, 12-14, NDVI, elevation
7	China	1772-1964	GARP	BIO 1, 2, 3, 7, 12, 14, 15
8	Qinghai-Tibetan Plateau, China	2004-2010	MaxEnt	Elevation, land surface temperature (day & night), NDVI, slope, aspect, land cover
9	Western USA	2000-2015	MaxEnt	BIO 1, 11, 16, 17, distances to grassland, shrubland, cropland, sparse vegetation, bare soil, artificial surface, probability of deer mouse, altitude

References

1. Nakazawa, Y. *et al.* Climate change effects on plague and tularemia in the united states. *Vector-borne and Zoonotic Diseases* **7**, 529–540 (2007).

2. Neerinckx, S. B., Peterson, A. T., Gulinck, H., Deckers, J. & Leirs, H. Geographic distribution and ecological niche of plague in sub-Saharan Africa. *International Journal of Health Geographics* **7**, 54 (2008).

3. Holt, A. C., Salkeld, D. J., Fritz, C. L., Tucker, J. R. & Gong, P. Spatial analysis of plague in California: niche modeling predictions of the current distribution and potential response to climate change. *International Journal of Health Geographics* **8**, 38 (2009).

4. Maher, S. P., Ellis, C., Gage, K. L., Enscore, R. E. & Peterson, A. T. Range-wide determinants of plague distribution in North America. *The American Journal of Tropical Medicine and Hygiene* **83**, 736–742 (2010).

5. Neerinckx, S. *et al.* Predicting potential risk areas of human plague for the Western Usambara Mountains, Lushoto District, Tanzania. *The American Journal of Tropical Medicine and Hygiene* **82**, 492–500 (2010).

6. Giles, J., Peterson, A. T. & Almeida, A. Ecology and geography of plague transmission areas in northeastern Brazil. *PLoS Neglected Tropical Diseases* **5**, e925 (2011).

7. Ben-Ari, T. *et al.* Identification of Chinese plague foci from long-term epidemiological data. *Proceedings of the National Academy of Sciences* **109**, 8196–8201 (2012).

8. Qian, Q. *et al.* Mapping risk of plague in Qinghai-Tibetan plateau, China. *BMC Infectious Diseases* **14**, 382 (2014).

9. Walsh, M. & Haseeb, M. Modeling the ecologic niche of plague in sylvan and domestic animal hosts to delineate sources of human exposure in the western United States. *PeerJ* **3**, e1493 (2015).